Journal of Materials Chemistry A

Accepted Manuscript

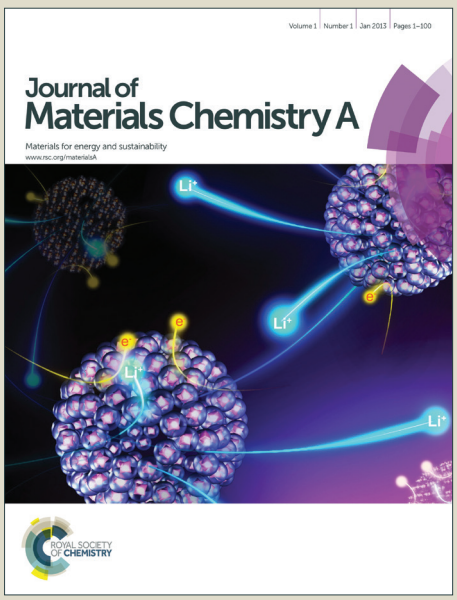

ROYAL SOCIETY OF CHEMISTRY

www.rsc.org/materialsA

Journal of
Materials Chemistry A

RSCPublishing

COMMUNICATION

Novel flower-like titanium phosphate microstructures and their application in lead ion removal in drinking water

Cite this: DOI: 10.1039/x0xx00000x

Received 00th January 2014,
Accepted 00th January 2014

DOI: 10.1039/x0xx00000x

www.rsc.org/

Xueyun Wang,[ab] Xiulin Yang,[ab] Jianhua Cai,[ab] Tingting Miao,[a] Lihua Li,[a] Gen Li,[a] Dingrong Deng,[a] Li Jiang,[*a] and Chunru Wang[a]

A novel flower-like $Ti(HPO_4)_2 \cdot H_2O$ microstructures were synthesized *via* a low-cost and credible method at low temperature. Assemble process was characterized with detail and possible formation mechanism of the hierarchical microstructures was clarified. The obtained products exhibit high surface area and excellent adsorption capacity for lead ions removal.

Heavy metal ions in water including Pb (II), Cd (II), and Hg (II) and so on are highly toxic water pollutants, which will seriously threaten local residents' health when their concentrations exceed permissible limits. However, a main challenge on drinking water treatment is the very low concentration of heavy metal ions comparing with other highly concentrated light-metal ions such Ca^{2+}, Mg^{2+}, Na^{+} etc.. It would be ideal if a technique can specifically remove the heavy metal ions free of light-metal ions influence with low-cost, high efficiency. In order to realize this target, scientists have developed many techniques such as membrane process,[1] electrochemical method,[2] chemical coagulation,[3] and adsorption,[4–11] etc. in the last decades, in which the adsorption technique has attracted essential attentions due to its cost-effectiveness and simplicity in operation.

For the adsorption technique in water treatment, the crux is to design and make high performance absorbents, e.g., metal oxides, metal silicates and metal hydroxide etc..[5,8–13] It was revealed that porous materials with three-dimensional hierarchically nanostructures usually exhibit high efficiency and special specificity to heavy metal ions due to their high surface area, facile mass transportation and abundant active adsorption sites. For example, hierarchically metal oxide nanostructures, flower-like α-Fe_2O_3 nanostructures, urchin-like α-FeOOH spheres, and porous TiO_2 spheres etc.,[14–16] have all shown remarkable removal capacity for heavy metal ions.

Titanium phosphates were known as high performance inorganic cation exchange materials,[17-23] and the alpha form titanium hydrogenphosphate, i.e., α-$Ti(HPO_4)_2 \cdot H_2O$, which owned layered, open-framework, and mesoporous structures with an interlayer distance of 0.76 nm, has been widely used in the field of water treatment to remove heavy metal ions.[17,23,24] Zhang *et al*. have employed amorphous titanium phosphate as ion-exchangers to remove Pb (II) and Cd (II) from water with capacity of 1.89 mmol g^{-1} (391.6 mg g^{-1}) and 0.558 mmol g^{-1} (62.72 mg g^{-1}) respectively.[23] Up to now, various methods such as layer by layer adsorption,[25] sol-gel and precipitation method[26,27] have been used to prepare $Ti(HPO_4)_2 \cdot H_2O$. However, few of these methods could synthesize $Ti(HPO_4)_2 \cdot H_2O$ with controllable morphologies, which are known to be critical for adsorption properties.

Here we report the preparation of uniform flower-like $Ti(HPO_4)_2 \cdot H_2O$ microstructures by a facile technique free of any surfactant or template. Typically, 500 μL tetrabutyl titanate was dissolved in 100 mL dehydrated alcohol and this mixture was stirred for 1 hour at room temperature. Then, 5 mL of 85% (w/w) phosphoric acid was added and stirred at 50 ^{o}C for 12 h. The suspension was then centrifuged and washed with distilled water and dried under vacuum at 50 ^{o}C.

The as-obtained $Ti(HPO_4)_2 \cdot H_2O$ microstructures showed a hierarchical flower morphology, which was examined by the field-emission scanning electron microscopy (FE-SEM) and transmission electron microscopy (TEM), as shown in Fig. 1. It could be observed that the microstructures were composed of numerous nanopetals with thickness of *ca.* 20 nm and width of *ca.* 1 μm, and the nanopetals connected with each other to self-assemble into three-dimensional flower-like hierarchical structures.

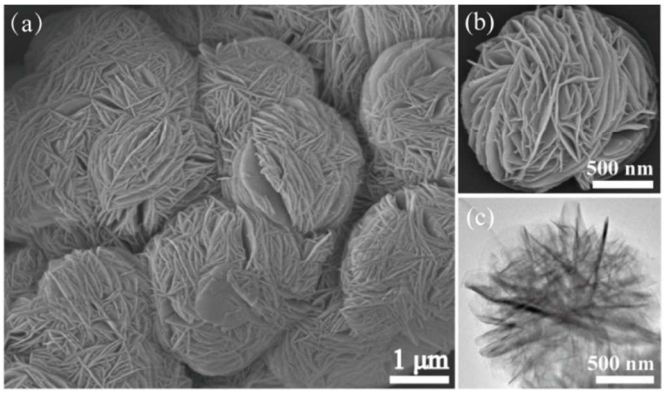

Fig. 1 (a) Typical SEM images of the prepared titanium phosphates. (b) High resolution SEM and (c) TEM image of the single flower-like structure of the titanium phosphate.

To investigate the formation process of the three dimensional hierarchical structures, time-dependent experiment was performed, in which samples were collected at different time intervals from the reaction mixture and studied by SEM to monitor the intermediates and products, as shown in Fig. 2. At the initial stage, in which nuclei formed and grew and the sample was composed of nanoflakes with diameters of ca. 100 nm (Fig. 2). As reaction proceeded, the nanoflakes continuously grew to ca. 200 nm and meanwhile new nanopetals began to grow on the surface of the nanoflakes as shown in Fig. 2b. Along with the reaction going on, more nanopetals grew on the flakes and connected to each other to form three-dimensional structure (Fig. 2c). The size of the three-dimensional nanostructure kept going up gradually and the morphology became flower-like composed of hundreds of petals as shown in Fig. 2d. The flower-like samples revealed interior net-like structures as shown in Fig. S1, which result in mesoporous structure and high surface area. For clarity, the morphological evolution process of $Ti(HPO_4)_2{\cdot}H_2O$ flower-like structures was illustrated in Fig. 2e, indicated a hierarchical nucleation and growth mechanism. Initially, nanoflakes nanonuclei were formed in solution at the original reaction stage. The nanoflakes then grew and served as nucleation centres to anchor the subsequent adsorbed reactors. After prolonged reaction, the adsorbed reactors further nucleated and grew to form nanopetals on the surface of the previously formed nanoflakes. With the reaction going on, each previous nanoflakes kept growing up and new nanopetals kept adhering till the complete three dimensional flower-like structures formed.

The as-obtained microstructures were studied by the XRD spectrometry, as shown in Fig. 3, which confirmed the composition of the microstructures was titanium phosphate with a formula of $Ti(HPO_4)_2{\cdot}H_2O$ (JCPDS card no. 80−1067). No peaks from impurities were detected by XRD. Moreover, the peak observed at higher 2θ corresponding to (0 0 2) peak and an interlayer spacing of 0.76 nm, indicated a layered structure of the sample. The broad peaks revealed small grain size and low crystallinity of the sample.

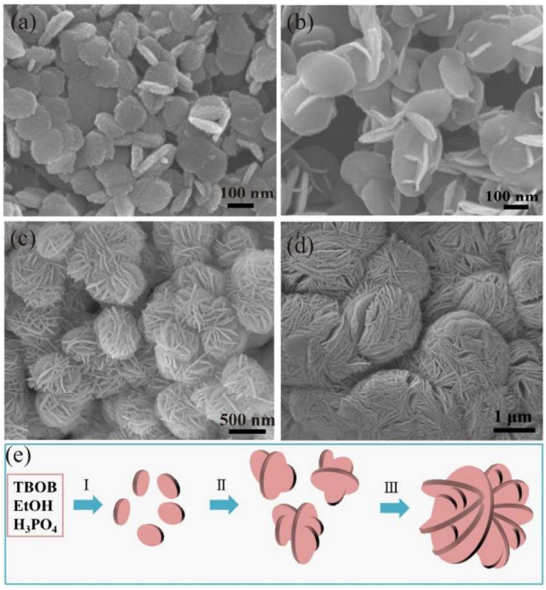

Fig. 2 SEM images of the nanostructures collected at different reaction time once the H_3PO_4 was added (a) 40min; (b) 1.5 h; (c) 5 h; (d) 12 h; (e) Schematic illustration of the formation process of the $Ti(HPO_4)_2{\cdot}H_2O$ nanostructures.

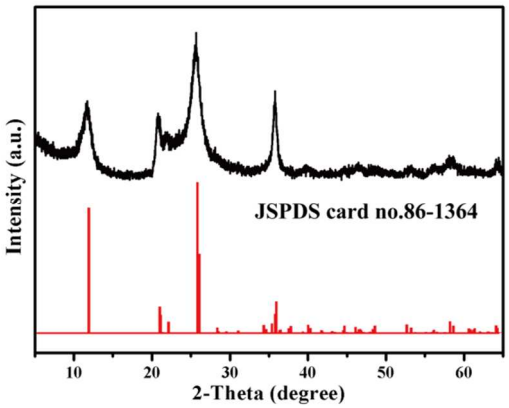

Fig. 3 XRD patterns of the flower-like $Ti(HPO_4)_2{\cdot}H_2O$.

Fascinatingly, detailed SEM studies revealed that the formation rates of $Ti(HPO_4)_2{\cdot}H_2O$ hierarchical structures depended strongly on the reaction temperature. As shown in Fig. S2, the forming time of $Ti(HPO_4)_2{\cdot}H_2O$ hierarchical structures changed from 48 hours at 30 ºC to 12 hours at 50 ºC and further to only 20 minutes at 80 ºC. Moreover, further XRD studies exhibited that the component of the hierarchical structures relied heavily on the reaction time. Once the $Ti(HPO_4)_2{\cdot}H_2O$ hierarchical structures formed, the reaction should be broken off in time, otherwise unwanted reaction products might be produced. For example, $Ti(HPO_4)_2{\cdot}H_2O$ hierarchical structures were observed to form in 12 hours at 50 ºC. However, when the reaction continued for more than 48 hours, the products would be transformed to $TiH_2(PO_4)_2{\cdot}2H_2O$ gradually, as shown in Fig. S3.

Fig. 4a showed the FTIR spectra of the $Ti(HPO_4)_2{\cdot}H_2O$ hierarchical structures. The broad band at about 3400 cm^{-1} and sharp peak at 1630 cm^{-1} corresponded to surface-adsorbed water and hydroxyl groups. The intense band around 1080 cm^{-1} was assigned to the P−O stretching mode. As for the peak

around 616 cm^{-1}, it could be assigned to the Ti–O band variation in the Ti–O–P matrix.[18,23] On the whole, the FTIR data confirmed that the phosphorus was incorporated into the framework in the form of Ti–O–P bonds. Fig. 4b depicted the TG curve of titanium phosphate, which showed two definite steps, as shown in following processes:

$$Ti(HPO_4)_2{\cdot}H_2O \xrightarrow[50\text{-}250\ ^oC]{-H_2O} Ti(HPO_4)_2 \xrightarrow[250\text{-}700\ ^oC]{-H_2O} TiP_2O_7$$

Where the first stage occurred between 50 and 250 ºC with a 9% mass loss was ascribed to loss of the hydrate water, and the second stage ranging from 250 to 700 ºC attributed to the loss of lattic water in composition of $Ti(HPO_4)_2{\cdot}H_2O$ resulting in the formation of titanium pyrophosphate. The total mass loss from the sample is nearly 16.7%. XRD patterns of the sample calcined at 250 ºC and 700 ºC (Fig. S4) confirmed the two stage weight loss process of $Ti(HPO_4)_2{\cdot}H_2O$ during thermogravimetric analysis.

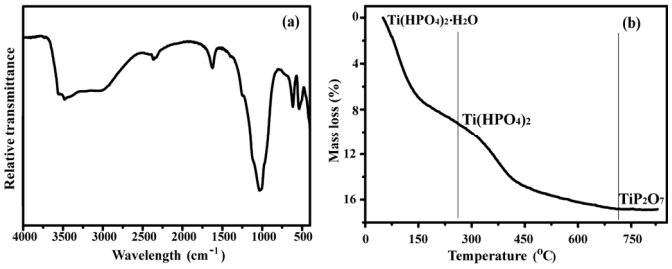

Fig. 4 (a) FTIR spectra and (b)Thermogravimetric (TG) of titanium phosphate

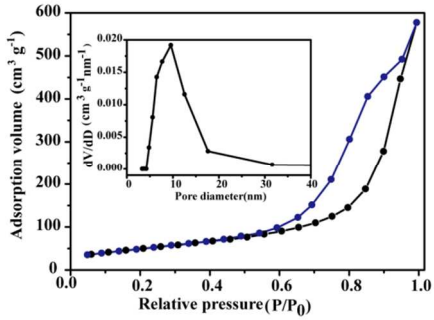

Fig. 5 Nitrogen adsorption/desorption isotherm of titanium phosphate.

The nitrogen adsorption/desorption isotherm of the titanium phosphate material shown in Fig.5 was of type IV and exhibits type H3 hysteresis loop at high relative pressure region. The corresponding pore size distribution of the sample took on narrow as shown in the inset of Fig. 5. Such a type of isotherm and hysteresis revealed the mesoporous structures of the materials with a high capacity of adsorption. The H3 type hysteresis loop also suggested the mesoporous structures were of parallel walls and open slit-shaped capillaries, which was usually observed in the aggregates with plate-like composite structure.[28] The material showed a BET surface area of 122m^2 g^{-1} and a total pore volume of 0.66 cm^3g^{-1}. Combining with the SEM characterization of inner of the sample (Fig. S1), it could be inferred that the high surface area and large total pore volume of the sample mainly generated from the interspaces of the nanopetals.

Due to the mesoporous hierarchical structure and ion-exchange property of $Ti(HPO_4)_2{\cdot}H_2O$, it is expected that this materials should own high adsorption capacity for heavy metal ions. The excellent ion-exchange property of $Ti(HPO_4)_2{\cdot}H_2O$ derived mainly from the HPO_4^- groups that can exchange with heavy metal ions. To elucidate the nature and numbers of exchangeable sites in $Ti(HPO_4)_2{\cdot}H_2O$, pH titration of the sample was firstly carried out and the results were depicted in Fig. S5a. Hydrogen ions within $Ti(HPO_4)_2{\cdot}H_2O$ were released in a continuous and stepwise manner. This is mainly because the acid groups within it are weakly dissociated and averse to exchange its H^+ ion for Na^+.[23,29] it is worth noting that only half of the exchangeable hydrogen ions (~3.94 mmol/g) within the adsorbent undertake ion exchange under neutral or weakly acidic conditions. The rest can only be released under alkaline condition in which most of the heavy metal ions are precipitated. Thus, the conceptual mechanism of heavy metal adsorption by $Ti(HPO_4)_2{\cdot}H_2O$ may be described as $Ti(HPO_4)_2{\cdot}H_2O + (1/2/)\ M^{2+} \leftrightarrow TiM_{1/2}H(PO_4)_2{\cdot}H_2O + H^+$, where M represents the corresponding heavy metal element.[23,29] Moreover, surface charge properties was a critical factor that relative to the adsorption capacity of an adsorbent. Thus, zeta potentials with changes of the pH of the solution were further investigated and the results were displayed in Fig. S5b. The surface of $Ti(HPO_4)_2 \cdot H_2O$ was highly negatively charged, which can prevent the particles aggregation due to electrostatic repulsion between them and will be beneficial to attract positively charged heavy metals. The effect of pH on the Pb^{2+} adsorption was examined and the results are presented in Fig. S5c. It can be found that the percentage of Pb^{2+} removal kept very high (> 98%) in a wide pH range (> 4) and still remained ~78.8% removal percentage even at pH=3, indicates wide pH operating range and high capability for Pb^{2+} removal of the as-prepared adsorbent.

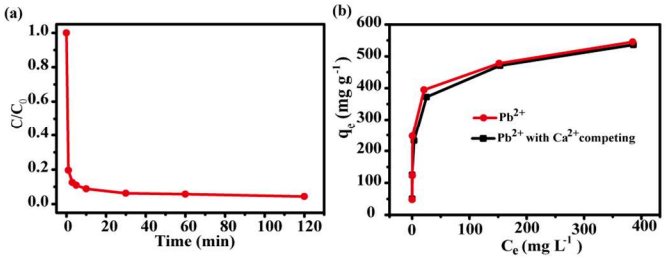

Fig. 6 (a) adsorption rates curves of Pb^{2+}, the initial ion concentration is 50 mg L^{-1} and sample dose is 20 mg/100 mL. (b) adsorption isotherms of Pb^{2+} with flower-like titanium phosphate nanostructures as adsorbents, the the initial ion concentration is 10~500 mg L^{-1} and sample dose is 5 mg/25 mL, the concentration of competition Ca^{2+} is 500 mg L^{-1}.

A simple experiment was designed for $Ti(HPO_4)_2{\cdot}H_2O$ hierarchical structures to remove lead ions in drinking water treatment, which is one of the most toxic aqueous heavy metal cations, and their efficient removal is vital for safe drinking water.

As shown in Fig. 6a, the adsorption rates of Pb^{2+} ions with an initial concentration of 50 mg L^{-1} on the absorbents were studied. It was observed that the adsorption processes proceeded very fast and the adsorption equilibrium was achieved within 1 h. Fig. 6b showed the adsorption isotherms of $Ti(HPO_4)_2{\cdot}H_2O$ hierarchical structures for Pb^{2+} ions with an adsorption capacity as high as 550 mg g^{-1}, which was much higher than those previously reported phosphate compounds.[23,29] Obviously, the enhanced performance of the as-prepared flower-like titanium phosphate could be attributed to the hierarchical structure with high BET surface area and large pore volume that provide much more active sites for heavy metal adsorption through ion exchanging or electrostatic interactions.

It should be noted that many coexisting high-concentrated cations such as Ca^{2+}, Mg^{2+}, Na^{+} etc. in drinking water, which may lead to the inefficiency of uptake of heavy metal ions in practical water treatment.[30] Therefore, Ca^{2+} was selected as a competitive cation to test its effect on the adsorption of Pb^{2+} by titanium phosphate. As shown in Fig. 6b, it is observed that the removal capacity of Pb^{2+} by $Ti(HPO_4)_2{\cdot}H_2O$ hierarchical structures was affected only slightly with the addition of Ca^{2+} ions (500 mg L^{-1}), revealing the super selectivity for Pb^{2+} removal. The high selectivity for Pb^{2+} removal of $Ti(HPO_4)_2{\cdot}H_2O$ hierarchical structures may be qualitatively interpreted by the hard and soft acids and bases (HASB) theory.[31-33] In aqueous solution, Pb^{2+} is much softer than Ca^{2+} and acts as borderline Lewis acid, so it possesses a higher priority to interact with the orthophosphate ion that serves as a borderline Lewis base. The XRD patterns of the samples after the metal uptake and HCl regeneration were shown in Fig. S6, indicated that the layered structure of $Ti(HPO_4)_2{\cdot}H_2O$ was capable of regenerating. ICP analysis showed that there is about 3.7 wt% of Pb^{2+} remaining in H^{+} treated absorbents. As shown in Fig. S7, the average concentrations of the titanium and phosphate released in treated water with different Pb^{2+} concentrations are 0.08 ppm and 3.42 ppm respectively, both of which are below the limit of the drinking water standard, revealing that the flower-like titanium phosphate is a safe adsorbent for lead ions in water.

Conclusions

In summary, a low cost and surfactant-free method was developed to synthesize novel mesoporous $Ti(HPO_4)_2{\cdot}H_2O$ hierarchical structures, which owns a large surface area of 122 m^2 g^{-1} and a large total pore volume of 0.66 cm^3 g^{-1}. When this material was used to remove lead ions, the removal capacity was revealed to be as high as 550 mg g^{-1} for lead ions. Moreover, the high efficiency for Pb^{2+} ion removal of the $Ti(HPO_4)_2{\cdot}H_2O$ hierarchical structures was maintained under the presence of high concentrated Ca^{2+} ions.

This work is supported by the National Natural Science Foundation of China (No. 21121063, 21273006, 61227902) and National Basic Research Program (No. 2011CB933700, 2012BAJ25B08).

Notes and references

[a] *Laboratory of Molecular Nanostructure and Nanotechnology, Institute of Chemistry, Chinese Academy of Sciences, Beijing 100190, China. jiangli@iccas.ac.cn.*

[b] *Graduate School of the Chinese Academy of Sciences, Beijing 100049 China.*

† Footnotes should appear here. These might include comments relevant to but not central to the matter under discussion, limited experimental and spectral data, and crystallographic data.
Electronic Supplementary Information (ESI) available: [details of any supplementary information available should be included here]. See DOI: 10.1039/c000000x/

1. C. Blocher, J. Dorda, V. Mavrov, H. Chmiel, N. K. Lazaridis and K. A. Matis, *Water Res.*, 2003, **37**, 4018-4026.
2. J. Song, H. Oh, H. Kong and J. Jang, *J Hazard. Mater.*, 2011, **187**, 311-317.
3. A. G. El Samrani, B. S. Lartiges and F. Villieras, *Water Res.*, 2008, **42**, 951-960.
4. Y. H. Ni, K. Mi. C. Cheng, J. Xia, X. Ma, J. M. H. *Chem. Commun.*, 2011, **47**, 5891.
5. C. Y. Cao, J. Qu, F. Wei, H. Liu and W. G. Song, *ACS Appl. Mater. Interfaces*, 2012, **4**, 4283-4287.
6. C.Y. Cao, P. Li, J. Qu, Z. F. Dou, W. S. Yan, J. F. Zhu, Z. Y. Wu and W. G. Song, *J. Mater. Chem.*, 2012, **22**, 19898.
7. H. Li, W. Li, Y. Zhang, T. Wang, B. Wang, W. Xu, L. Jiang, W. Song, C. Shu and C. Wang, *J. Mater. Chem.*, 2011, **21**, 7878.
8. J. S. Hu, L. S. Zhong, A. M. Cao, Q. Liu, W. G. Song, and L. J. Wan, *Chem. Mater.*, 2007, **19**, 1648 - 1655.
9. Y. Ide, N. Ochi and M. Ogawa, *Angew. Chem. Int. Ed.*, 2011, **50**, 654-656.
10. N. Wu, H. Wei and L. Zhang, *Environ. Sci. Technol.*, 2012, **46**, 419-425.
11. M. C. Kimling and R. A. Caruso, *J. Mater. Chem.*, 2012, **22**, 4073.
12. J. Qu, C. Y. Cao, Y. L. Hong, C. Q. Chen, P. P. Zhu, W. G. Song and Z.-Y. Wu, *J. Mater. Chem.*, 2012, **22**, 3562.
13. K. H. Goh, T. T. Lin. Z. L. Dong, *Environ. Sci. Technol.*, 2009, **43**, 2537-2543.
14. L. S. Zhong, J. S. Hu, H. P. Liang, A. M. Cao, W. G. Song and L. J. Wan, *Adv Mater*, 2006, **18**, 2426-2431.
15. B. Wang, H. Wu, L. Yu, R. Xu, T. T. Lim and X. W. David Lou, *Adv Mater,* 2012, **24**, 1111−1116.
16. L. S. Zhong, J. S. Hu, L. J. Wan and W. G. Song, *Chem. Commun.*, 2008, **0**, 1184−1186.
17. Liliane M. Nunes, Bruno Parente, Maria A. M. Maurera, and Claudio Airoldi , *Ind. Eng. Chem. Res.*, 2008, **47**, 5441-5446.
18. A. Bhaumik,S. Inagaki , *J. Am. Chem. Soc.*, 2001, **123**, 691 - 696.
19. A. Dutta, A. K. Patra, S. Dutta, B. Saha and A. Bhaumik, *J. Mater. Chem.*, 2012, **22**, 14094.
20. D. J. Jones, G. Aptel, M. Brandhorst, M. Jacquin, J. Jiménez-Jiménez, A. Jiménez-López, P. Maireles-Torres, I. Piwonski, E. Rodríguez-Castellón, J. Zajac and J. Rozière, *J. Mater. Chem.*, 2000, **10**, 1957−1963.
21. H. Takahashi, T. Oi and M. Hosoe, *J. Mater. Chem.*, 2002, **12**, 2513-2518.
22. X. J. Z. T. Y. Ma, G. S. Shao, J. L. Cao, and Z. Y. Yuan, *J. Phys. Chem. C*, 2008, **112**, 3090-3096.
23. K. Jia, B. Pan, Q. Zhang, W. Zhang, P. Jiang, C. Hong, B. Pan and Q. Zhang, *J. Colloid. Interf. Sci.*, 2008, **318**, 160−166.

24. A. I. Abraham Clearfield , Sergei A. Khainakov ,Lyudmila N , Vladimir V. Strelko , Vladimir N. Khryaschevskii, *Waste Manage.,* 1998, **18**, 203-210.
25. Q. F. Wang, L. Zhong, J. Q. Sun, and J. C. Shen, *Chem. Mater.*, 2005, **17**, 3563-3569.
26. J. Zhang, Z. Ma, J. Jiao, H. Yin, W. Yan, E. W. Hagaman, J. Yu and S. Dai, *Langmuir*, 2009, **25**, 12541−12549.
27. C. Pan, S. Yuan and W. Zhang, *Appl. Catal., A.*, 2006, **312**, 186−193.
28. J. L. Gunjakar, T. W. Kim, H. N. Kim, I. Y. Hwang, S. J. Hwang, *J. Am. Chem. Soc.*, 2011, **133**, 14998−15007.
29. Q. R. Zhang, W. Du, B. C. Pan, B. J. Pan, W. M. Zhang, Q. J. Zhang,Z. W. Xu and Q. X. Zhang, *J. Hazard. Mater.*, 2008, **152**, 469-475. 30. Li, N.; Zhang, L.; Chen, Y.; Fang, M.; Zhang, J.; Wang, H. Adv. Funct. Mater., 2012, **22**, 835-841.
31. R. G. Pearson, J. Am. Chem. Soc. 1963, **85**, 3533-3539.
32. R. G. Pearson, J. Chem. Educ. Ion. 1968, **45**, 581-587.
33. R. G. Pearson, J. Chem. Educ. Ion. 1968, **45**, 643-648.